



# Remaining useful life prediction of reaction wheel motor in satellites

Yuri Yun<sup>1</sup> · Junyong Lee<sup>1</sup> · Hwa-suk Oh<sup>2</sup> · Joo-Ho Choi<sup>2</sup>

Received: 31 July 2018 / Revised: 31 March 2019 / Accepted: 20 May 2019 / Published online: 3 July 2019  
© The Author(s) 2019

## Abstract

For advanced attitude control of the satellite, reaction wheels are used, which are actuated by motor. Fault detection and prediction of Remaining Useful Life (RUL) of the motor is of great importance. This study aims to demonstrate health management of reaction wheel motor in satellites by estimating the RUL of the damping coefficient. Multi-scale Extended Kalman Filter (EKF) is employed for this purpose using the data of input current and output velocity measured during the life test of the motor. The motor dynamic behavior is modeled by the ordinary differential equations. The damping coefficient is taken as the health indicator, which is obtained by solving the micro EKF problem. To set threshold for the damping coefficient, degradation behavior of characteristic curve that evaluates the motor performance is used to correlate with the degradation of the damping coefficient. Then, the RUL is predicted by solving the macro EKF problem.

**Keywords** Remaining useful life (RUL) · Prognostics and health management (PHM) · Ordinary differential equations (ODEs) · Motor · Multi-scale extended Kalman filter (EKF) · Damping coefficient

## 1 Introduction

For very accurate attitude control systems and for moderately fast maneuvers in the satellite operation in space, reaction wheels are preferred because they allow continuous and smooth control. Reaction wheel is used as an actuator to control the attitude of a satellite using the reaction torque generated when the inertia and speed of the wheel attached to the motor shaft are changed [1]. The motor used to control the reaction wheel is given in the circle of Fig. 1, which is Brushless direct current (BLDC) type, and torque is generated by Lorentz's force law which is the combination of electric and magnetic force due to electromagnetic fields [2]. The function of the motor usually degrades because the damping coefficient increases over the repeated use in operation cycles. To ensure the reliable operation and prevent unwanted failure of the reaction wheel, fault detection and life prediction of the motor during the operation is of great importance.

In the previous literature, there have been only a few studies for the prognosis of motor that predicts the life during the operation, whereas many are available for the diagnosis. Lim et al. [3] estimated the failure mode and mechanism based on the FMEA and QFD through failure cases that occur in the field and suggested a method to predict failure using the frequency amplitudes after FFT as the degradation feature. Li et al. [4] presented a method of life prediction for DC motor using the time series modeling procedure of the measured voltage based on the accelerated testing data. Zheng et al. [5] studied life prediction of induction motors based on a simple accelerated degradation testing method. The life and reliability of the motor is finally predicted and evaluated using the Weibull distribution and Maximum Likelihood Estimations (MLE). Previous studies, however, are mostly based on the data-driven approach, which is to extract degradation features from empirical or intuitive reasoning and hence, are of limited value in terms of physical interpretation.

In this study, a model-based approach is used to real-time diagnose the condition of the motor and predict the Remaining Useful Life (RUL) until failure, based on the accumulated data up to the current cycle. Damping coefficient of the motor is used as the health feature, because the motor performance, which degrades gradually over cycles, is largely affected by the damping coefficient. Multi-scale Extended Kalman Filter (EKF) method is employed to achieve this

✉ Joo-Ho Choi  
yuri.yun@kau.kr

<sup>1</sup> Department of Aerospace and Mechanical Engineering, Korea Aerospace University, Goyang, Gyeonggi-do, Korea

<sup>2</sup> School of Aerospace and Mechanical Engineering, Korea Aerospace University, Goyang, Gyeonggi-do, Korea

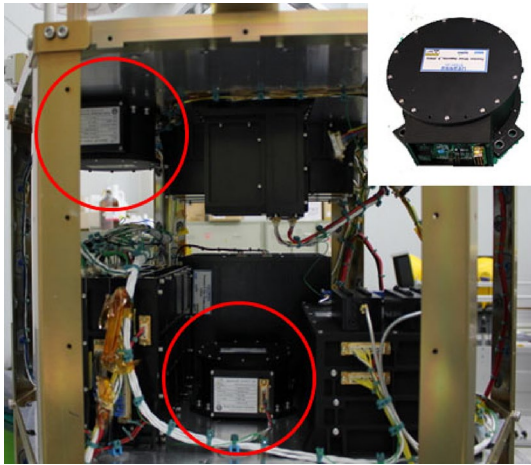


**Fig. 1** A motor from Korea Space Launch Vehicle-I

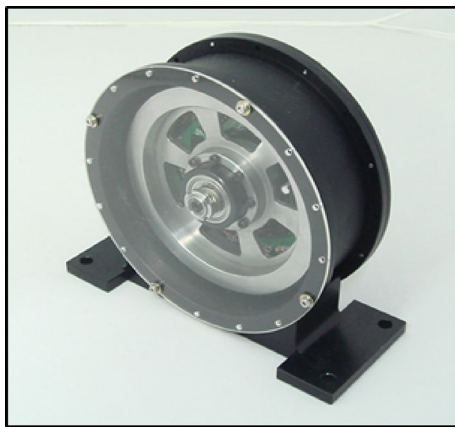


**Fig. 2** SRB-361-1103 Motor

objective: First, damping coefficient is estimated based on the real-time motor measurements at each cycle using the micro EKF, in which the motor dynamics is given by the ordinary differential equations (ODEs) [6]. Next, degradation behavior is estimated based on the damping coefficient accumulated up to the current cycles and extrapolated to the failure level using the macro EKF [7]. In order to examine the feasibility of the method, the data measured throughout the life cycle test of the motor are used under the wheel speed control mode.

## 2 Experiment

The motor used to control reaction wheel is given in Fig. 2, whose specifications are described in Table 1. The motor has both electric and mechanical characteristics, and one can check the performance of these by carrying out a pull-up and

**Table 1** Motor specifications

	SRB-361-1103
Angular momentum @ nom. Speed	0.36 Nms
Physical dimensions	
Diameter	139 mm
Height	51.5 mm
Total mass	1.38 kg
Wheel inertia	0.001143 kg m <sup>2</sup>
Torque constant	0.0568 Nm/A
Back-emf constant	0.0568 Nm/A
Friction coefficient (bearing)	$1.01 \times 10^{-5}$ (Bearing: 6000)
Friction coefficient (air drag)	$0.72 \times 10^{-5}$
Current	(24 V)
Steady state @ 3000 rpm	0.19 A

**Fig. 3** Thermal vacuum chamber (TC-65P)



run-down test, respectively. Pull-up test works by applying maximum voltage to the motor and check the electrical performance. Run-down test is used to examine the mechanical performance of the wheel. The test is repeated until failure, during which the performance of the motor is periodically measured. In this study, the data are gathered during the pull-up test, which consists of time, input current and output angular velocity, and acceleration occurred as a result of maximum voltage application. The test is carried out to evaluate the reliability and performance in the satellites over 3 years (2013.11.19~2016.12.03) under hot (60 °C) condition in the thermal vacuum chamber as shown in Fig. 3. The data measured over a cycle are illustrated in Figs. 4, 5 and 6. Note that the reason to apply the peak of input current at its initial stage as shown in Fig. 4 is to impose the extreme condition to the motor during the cycle.

## 3 Multi-scale EKF process

Overall framework of the multi-scale EKF is given in Fig. 7, which consists of two steps: on-line damping estimation and off-line trend monitoring. In on-line damping estimation, the

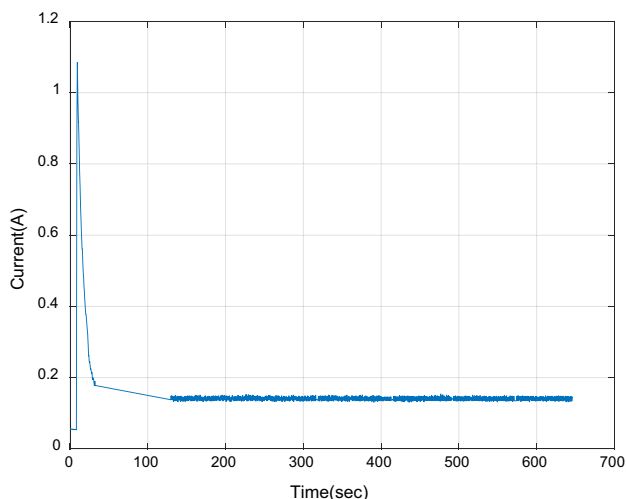


Fig. 4 Input current applied to the motor in a cycle

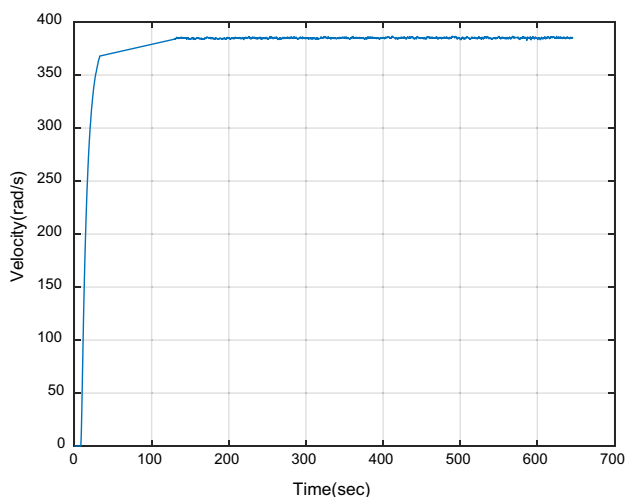


Fig. 5 Measured angular velocity in a cycle

damping coefficient is estimated based on the real-time motor measurements within a single cycle by the micro EKF, while in off-line trend monitoring, the degradation parameter is estimated based on the damping coefficient accumulated up to the current cycles by the macro EKF.

### 3.1 On-line damping estimation by micro EKF

First step is the on-line damping estimation, in which the damping coefficient is estimated based on the real-time motor measurements within a single cycle by the micro EKF. The governing equation of the motor dynamics is given as follows:

$$T_{gen} = J \cdot \dot{w} + c \cdot w + T_L, \tag{1}$$

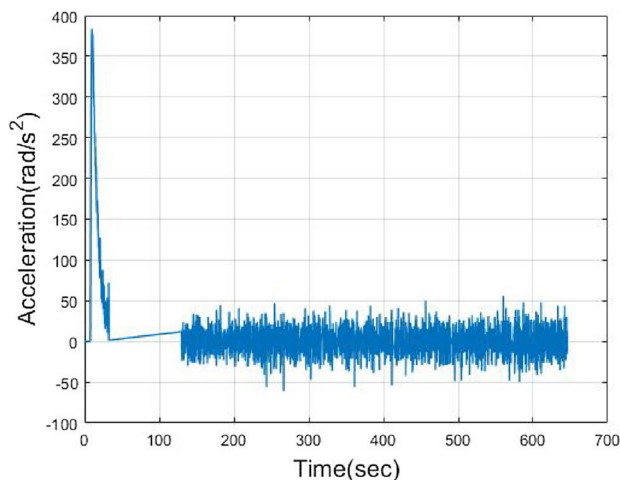


Fig. 6 Measured angular acceleration in a cycle

where  $T_{gen} = KI$  is the input torque given by the input current  $I$ ,  $K$  is the torque constant,  $J$  is the motor inertia,  $w$  is the angular velocity of the motor,  $\dot{w}$  is its acceleration,  $c$  is the damping coefficient and  $T_L$  is the load torque given by the constant value, respectively. In the equation,  $T_{output} = J \dot{w}$  is defined additionally as opposed  $T_{gen}$  to evaluate the motor performance in the study.

To apply multi-scale EKF, Eq. (1) is transformed to the recursive formulation [8], in which the state and measurement equations are represented as follows:

$$\begin{aligned} x_k &= f(x_{k-1}, I_{k-1}) + q_{k-1} \\ z_k &= h(x_k) + v_k \end{aligned} \tag{2}$$

or

$$\begin{aligned} x_k &= \begin{bmatrix} \tilde{w}_k \\ \tilde{c}_k \end{bmatrix} = \begin{bmatrix} w_{k-1} + (-c_{k-1}w_{k-1} - T_L + KI_{k-1})dt/J \\ c_{k-1} \end{bmatrix} + q_{k-1} \\ z_k &= \begin{bmatrix} w_k \\ \dot{w}_k \end{bmatrix} = \begin{bmatrix} \tilde{w}_k \\ (-c_{k-1}\tilde{w}_{k-1} - T_L + KI_{k-1})/J \end{bmatrix} + v_k \end{aligned} \tag{3}$$

where the state variable vector  $x_k$  includes  $\tilde{w}_k$  and  $\tilde{c}_k$ , and the measurement variable  $z_k$  includes  $w_k$  and its acceleration  $\dot{w}_k$ . In the equations,  $k$  is the current time index,  $c$  is the health parameter, and  $q$  and  $v$  denote the noises in the system and measurement, respectively. The symbol  $\sim$  means the time update at the step  $k$  from the previous step  $k - 1$ .

The micro EKF for online damping estimation consists of two sub-steps as shown in Fig. 7: time update and measurement update. In the time update, the state variables are updated from the previous time step  $k - 1$  by the input current  $I_{k-1}$  at the current time step as shown in Fig. 4 for the duration of 650 s of a single cycle. Then they are corrected using the measured data  $z_k$  in the measurement update. As the measured velocity  $w_k$  and acceleration  $\dot{w}_k$  are given at each of the

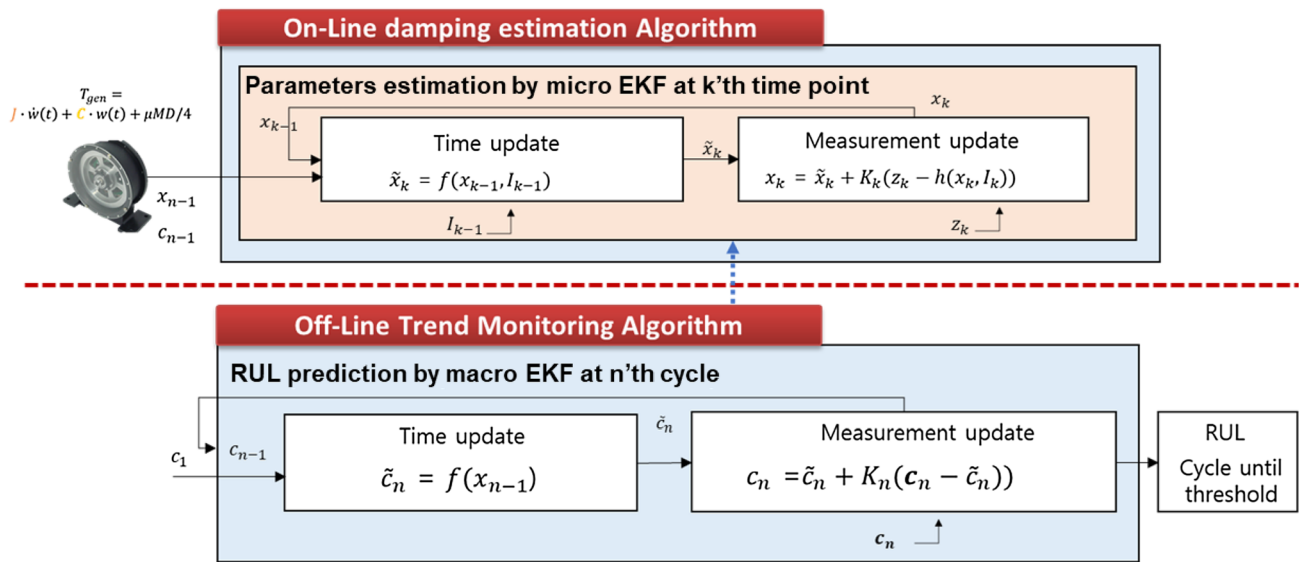


Fig. 7 Overall framework of the multi-scale EKF

sampled time as shown in Figs. 5 and 6; this is repeated recursively to get the final estimated values at the end of the cycle.

### 3.2 Off-line trend monitoring by macro EKF

Second step is the off-line trend monitoring, in which the parameter representing the damping degradation is estimated based on the accumulated data of estimated damping coefficient up to the current cycles by the macro EKF. In this step, the degradation of damping coefficient  $c$  is assumed by experience as a simple linear equation with respect to the cycles as follows:

$$c(t) = c_0 + a \cdot t \tag{4}$$

where  $c$  is the damping coefficient,  $t$  is number of cycles, and coefficient  $a$  is the slope determined using the macro EKF. Equation (4) can also be transformed to the recursive form to implement EKF. The state and measurement model are then given, respectively, as follows:

$$\begin{aligned} x_n &= f(x_{n-1}) + q_n \\ z_n &= h(x_n) + v_n \end{aligned} \tag{5}$$

or

$$\begin{aligned} x_n &= \begin{bmatrix} \tilde{c}_n \\ \tilde{a}_n \end{bmatrix} = \begin{bmatrix} \tilde{c}_{n-1} + a_{n-1} \cdot dt \\ a_{n-1} \end{bmatrix} + q_{k-1} \\ z_n &= \tilde{c}_k + v_n \end{aligned} \tag{6}$$

where the state variable  $x_n$  includes the damping coefficient  $c_n$  and its degradation slope  $a_n$ . The measurement variable  $z_n$  is the updated damping coefficient, which was obtained

from the micro EKF. The EKF matrices in this step are given as follows:

$$\begin{aligned} F &= \frac{\partial f}{\partial x} = \begin{bmatrix} 1 & dt \\ 0 & 1 \end{bmatrix} \\ H &= \frac{\partial h}{\partial x} = \begin{bmatrix} 1 & 0 \end{bmatrix} \end{aligned} \tag{7}$$

As the damping coefficient is given one at a cycle from the micro EKF, the state of the model and its unknown slope is estimated based on the macro EKF. Then the model is used to predict the RUL for the unrealized future cycles.

## 4 Results of multi-scale EKF

### 4.1 Estimation of damping coefficient by micro EKF

In this section, the damping coefficient is estimated at each cycle using the micro EKF as a short-term diagnosis. The results are given in Fig. 8 as an illustration, which represents the estimated mean and 95% confidence bounds of the state variables: the velocity and the damping coefficient in a cycle. Note that the duration of a single cycle is not constant but varies from cycle to cycle, ranging between the minimum of 170 up to the maximum of 100,000 s. For the damping coefficient in the cycle, the mean at the end is used as the representative value of the cycle, which is used as the value in the degradation trending over cycles in the subsequent macro EKF. The values obtained at each cycle are plotted in terms of cycles in Fig. 9.

**Fig. 8** Estimated state variables with confidence bounds in a single cycle

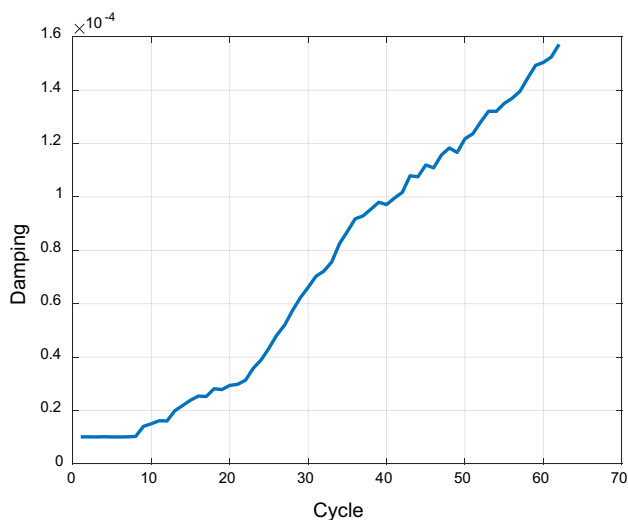
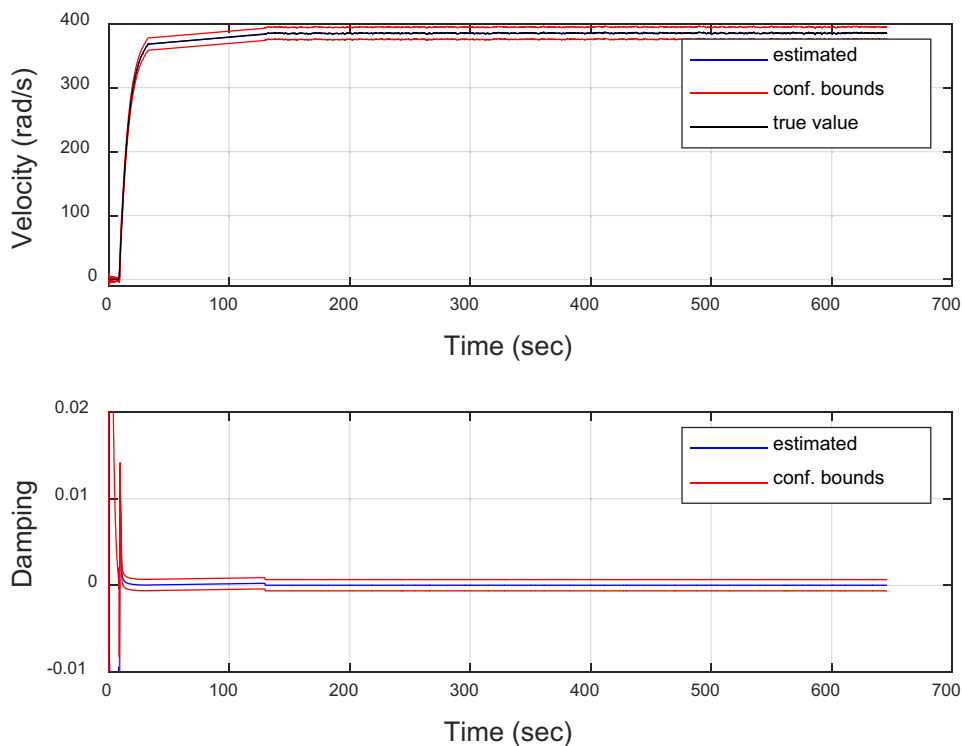


**Fig. 9** Damping coefficient degradation over cycles

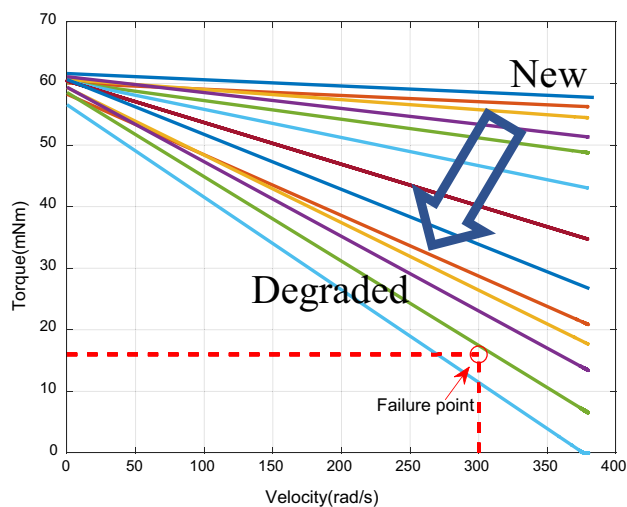


**Fig. 10** Characteristic curve of motor degrading over cycles

**4.2 Setting the threshold**

Once the state variable is estimated in a cycle by micro EKF, characteristic curve of the motor can be constructed, which is defined by the relation between the output torque as given by  $T_{output} = J \dot{\omega}$  and the angular velocity  $\omega$ . This is plotted in Fig. 10 for cycles with an increment of 5, in which the torque and velocity are given at y axis and x axis, respectively. It is noted that this curve is typically used to evaluate the motor performance degradation and to set the failure threshold in

the satellite research community. As shown in the figure, failure is declared if the curve falls beyond the critical point as specified by dotted red line assigned by the design during the degradation, which is 300 rad/s and 16 mNm. Since the health index in this study is damping coefficient of the motor, the characteristic curve at this condition is used to obtain critical value of the damping coefficient using which the RUL will be predicted. In order to relate this with the damping coefficient, the slope of the characteristic curve is exploited since it gradually increases to the negative

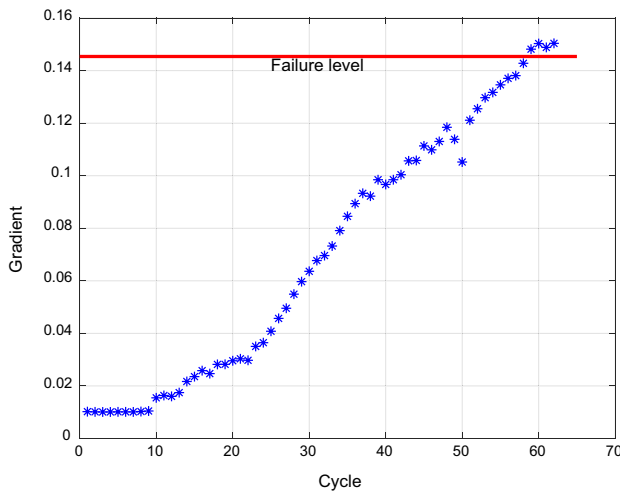


Fig. 11 Changes of gradient of characteristic curve

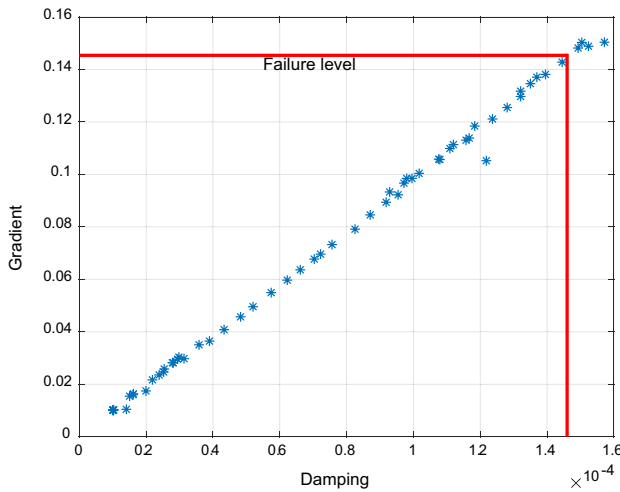


Fig. 12 Gradient versus damping coefficient

direction as shown in the arrow direction of Fig. 10, and as shown by the slope values increases over cycles in Fig. 11. Then the slope at the critical point of the characteristic curve is found to be 0.1428. Since both slopes of the characteristic curve and damping coefficient are increasing, their relation can be plotted in a graph as shown in Fig. 12. The corresponding damping coefficient at failure level is 0.000147, and this will be used for the RUL prediction in the subsequent macro EKF.

### 4.3 Prediction of RUL by macro EKF

In this step, the state equation is the degradation model of the damping coefficient, which is assumed to increase linearly over the cycles. Measurement data are provided

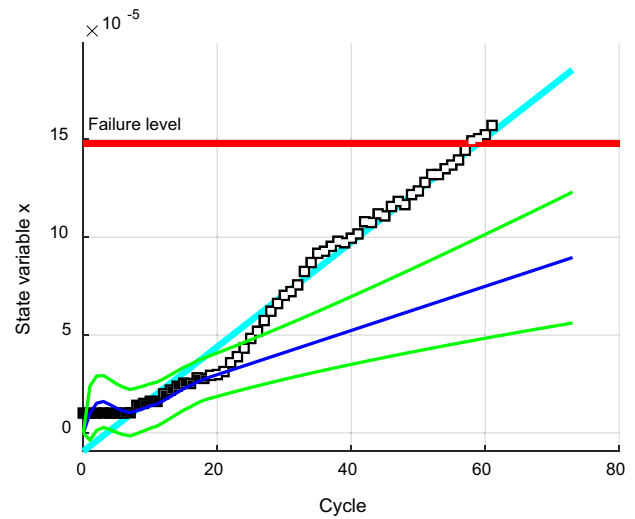


Fig. 13 RUL prediction of damping coefficient by macro EKF at 20th cycle

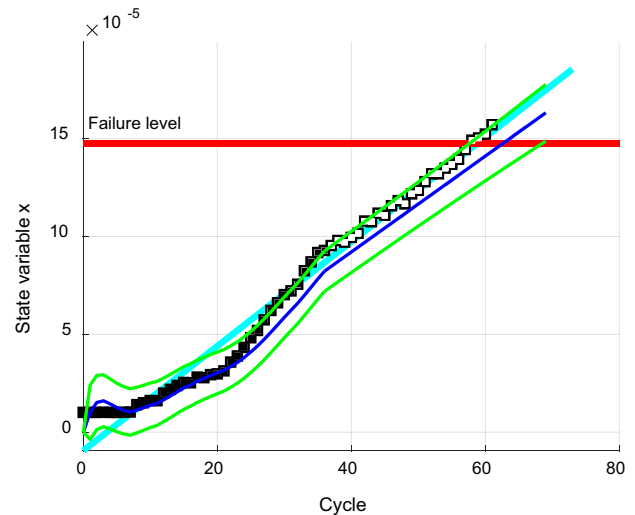
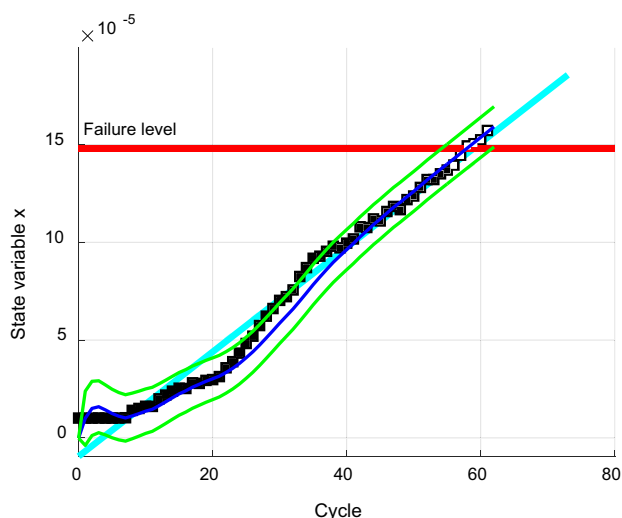


Fig. 14 RUL prediction of damping coefficient by macro EKF at 40th cycle

by the estimated coefficient from micro EKF. Then the coefficient value and the slope in the degradation model are estimated from the data given from the micro EKF up to the current cycles. RUL is then predicted along with the confidence bounds, which represents the remaining cycles until reaching failure threshold. Figures 13, 14 and 15 represent the estimation of the damping coefficient using the data up to the 20th, 40th and 58th cycle and prediction into the future from these cycles, respectively. The two green curves are their predictive intervals. As can be found, the more the measurement data are used, the more accurate the prediction with narrower interval achieved.





**Fig. 15** RUL prediction of damping coefficient by macro EKF at 58th cycle

The slope of the degradation model is estimated as shown in Fig. 16, in which the convergence of the slope is observed toward the value of  $2.67 \times 10^{-6}$  as the data are added over cycles. Using the failure threshold obtained in the previous section, the RUL is also predicted as shown in Fig. 17 as a function of cycles, in which the black line is true value, and the red curves are the predictive bounds of RUL. It is observed that the predictive bounds quickly narrow down as more data are introduced.

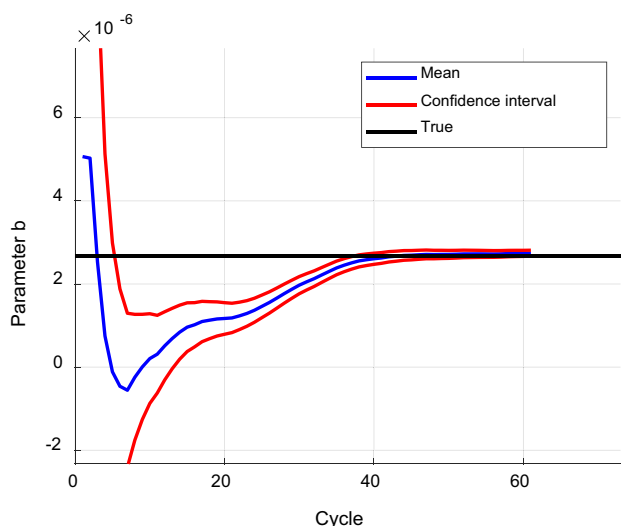


**Fig. 16** Estimation of slope in degradation model

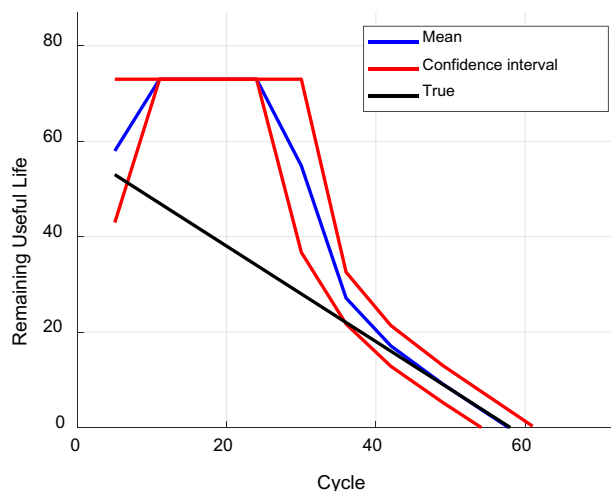


**Fig. 17** Estimation of RUL and comparison with true values

### 5 Conclusions

In this paper, prognostic process using the multi-scale EKF is developed and implemented to the real motor data of the reaction wheel in the satellite for long-term RUL prediction. Thus, by solving the micro and macro EKF problem based on the motor dynamics and linear degradation model of damping coefficient, it enables the RUL prediction and proactive action before the motor failure is encountered. Under the hot condition (60 °C), life prediction of the motors during the operation yields good results and damping coefficient is very good indicator. Present study has predicted motor life for constant hot condition. However, in the real space, the motor undergoes hot and cold condition alternatively in a single cycle. The method should be successfully applied to this condition. This will be studied in the future, which requires data for run-to-failure test under this condition.

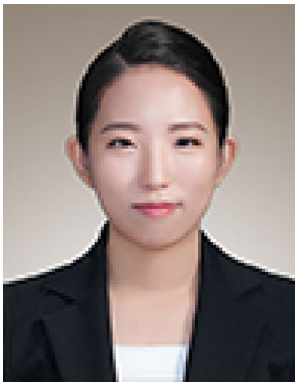
**Acknowledgements** This work was supported by the National Research Foundation of Korea (NRF) grant funded by the Korea government (MSIT) (No. 2016R1A2B4015241), and 2019 Korea Aerospace University Faculty Research Grant.

**Open Access** This article is distributed under the terms of the Creative Commons Attribution 4.0 International License (<http://creativecommons.org/licenses/by/4.0/>), which permits unrestricted use, distribution, and reproduction in any medium, provided you give appropriate credit to the original author(s) and the source, provide a link to the Creative Commons license, and indicate if changes were made.

### References

1. M.J. Sidi, *Spacecraft dynamics and control: a practical engineering approach*, vol. 7 (Cambridge University Press, Cambridge, 2000)

2. I. Boldea, S.A. Naser, *Linear Motion Electromagnetic Systems* (1985)
3. J. Lim, H.-W. Lim, Study on failure prediction method of BLDC motor driver. *J. Adv. Eng. Technol.* **9**(2), 105–109 (2016)
4. L. Wang, Z. Liu, H. Xue, B. Wan, Life prediction of DC motor using time series analysis based on accelerated degradation testing. *Res. J. Appl. Sci. Eng. Technol.* **6**(24), 4553–4558 (2013)
5. D. Zheng et al. Study on the life prediction of induction motors based on accelerated degradation testing method. in *2011 9th International Conference on Reliability, Maintainability and Safety (ICRMS)*, IEEE (2011)
6. V.A. Skormin, J. Apone, J.J. Dunphy, On-line diagnostics of a self-contained flight actuator. *IEEE Trans. Aerosp. Electron. Syst.* **30**(1), 186–196 (1994)
7. R. Xiong et al., A data-driven multi-scale extended Kalman filtering based parameter and state estimation approach of lithium-ion polymer battery in electric vehicles. *Appl. Energy* **113**, 463–476 (2014)
8. C. Hu, B.D. Youn, Jaesik Chung, A multiscale framework with extended Kalman filter for lithium-ion battery SOC and capacity estimation. *Appl. Energy* **92**, 694–704 (2012)



**Yuri Yun** received the B.S. and M.E degree of mechanical engineering from Korea Aerospace University in 2017 and 2019, respectively. On graduation she joins Hyundai Construction Equipment co, Ltd as a research engineer. Her current research is focused on the prognostics and health management for rotary machines.



**Junyong Lee** received his B.E. and M.E. degrees in Aerospace Engineering from Korea Aerospace University, Korea, in 2014 and 2016, respectively. He is currently a Ph.D. candidate at the same University. His research interest is developing attitude hardware such as reaction wheel, CMG, etc.



**Hwa-suk Oh** received his Ph.D. degree in Aerospace Engineering from Texas A&M University in 1992. After spending several years in ETRI in Korea, he is currently a professor of the School of Aerospace and Mechanical Engineering at Korea Aerospace University. His research interests include satellite attitude control and determination. Recent researches are concentrated into developing attitude hardware such as reaction wheel, CMG, MEMS IMU, etc.



**Joo-Ho Choi** received his B.S. degree of mechanical engineering from Hanyang University in 1981, M.S. degree and Ph.D. degree of mechanical engineering from Korea Advanced Institute of Science and Technology (KAIST) in 1983 and 1987, respectively. During the year 1988, he worked as a Postdoctoral Fellow at the University of Iowa. He joined the School of Aerospace and Mechanical Engineering at Korea Aerospace University, Korea, in 1997 and is now Professor. His current research is focused on the reliability analysis, design for life-time reliability, and prognostics and health management.